

Quantum Superposition State Production by Continuous Observations and Feedback

Antonio Negretti,* Uffe V. Poulsen, and Klaus Mølmer
Lundbeck Foundation Theoretical Center for Quantum System Research
Department of Physics and Astronomy, University of Aarhus
DK-8000 Aarhus C, Denmark
(Dated: October 4, 2018)

We present a protocol for generation of superpositions of states with distinguishable field amplitudes in an optical cavity by quantum non-demolition photon number measurements and coherent feeding of the cavity.

PACS numbers: 03.67.-a; 02.30.Yy; 42.50.Dv

By suitably tailored optical pulses it is possible to coherently manipulate the states of small quantum systems and for example to steer molecular processes and chemical reactions. Methods and concepts from this research have spread to the field of quantum information theory which, even with quantum error correction, requires a very high degree of control [1]. As an example, quantum optimal control techniques can substantially improve the performance of elementary quantum gates with cold neutral atoms [2]. Optimal control methods aim at manipulating a few external parameters, e.g., currents and magnetic fields of an atomic trapping potential, in such a way that an initial state of the system evolves into the desired final state with high fidelity. These techniques are open-loop, i.e., they do not exploit the knowledge that one can get by observing the system and using the measurement outcome in a suitable feedback. Even quite simple measurements display powers which are hard to match with controllable interactions in terms of the states accessible. For example, optical probing of spin-polarized macroscopic atomic samples has been used to enable atomic spin-squeezing [3], entanglement, quantum storage [4] and teleportation [5], and measurements of the phase of light transmitted through a modest cavity has been proposed as a means to project product states of atoms in the cavity into entangled states and to implement quantum computation [6].

The natural next step is to apply feedback continuously in time using the information acquired in real time with the measurements. The theory for continuous measurements and feedback [7, 8] combines the non-deterministic elements of quantum trajectories [9, 10] with stochastic calculus. While these theories describe correctly the outcome of a given measurement and feedback scheme, it is still an open problem how one identifies reliable schemes for a given task. A scheme for photon Fock state generation in a cavity has been proposed recently by Geremia in Ref. [11] and an analysis of the stability of the feedback by Yanagisawa [12]. In this Letter we propose a strategy to generate an equal superposition of two quantum-mechanical states with distinguishable field amplitudes $|\Psi\rangle \propto |A\rangle + |B\rangle$. Superpositions of states, which are well localized in separate regions of the effective position-

momentum phase space of the field variables, have been proposed as useful resources for quantum computation [13] and quantum metrology [14]. Other methods for generation of such superposition states have been demonstrated with light [15, 16] and with trapped ions [14]. Our principal idea is to apply the method described in Ref. [11] to approach a target Fock state, occupying a ring in the field amplitude phase space. Before we reach this state, the phase space distribution is of crescent shape [see Fig. 1(b)], and we feed coherent radiation into the cavity to displace the state [Fig. 1(c)]. We subsequently start probing the photon number again. In a pictorial representation, this scheme will select a quantum state with phase space support at the overlap of a new Fock state ring and the displaced crescent distribution, i.e., at two crossing regions, and hence a linear superposition of two quantum states with distinguishable field amplitudes may result from the protocol [Fig. 1(d)].

A quantum non-demolition measurement of the photon number \hat{n} in a single cavity mode can be accomplished by measuring the phase shift of a probe laser field that couples via a cross-Kerr effect to the cavity field when it passes through an atomic gas inside the cavity. In our simulations, we apply physical parameters of a dark-state mechanism in the gas for effective coupling of the fields taken from Ref. [11], but the formalism is general and describes also the effective coupling based on the collective atomic motion inside the cavity, studied in Ref. [17]. The interaction Hamiltonian is proportional to the product of the cavity and the probe photon number operators and it causes a phase shift of the probe without exchanging photons with the cavity field. It thus enables a non-demolition interaction which will gradually cause a narrowing of the photon number state distribution. Our simulations will apply the stochastic master equation technique [7, 11], but in order to explain this method and to get useful insight, it is worthwhile to establish a simple physical picture of the underlying probing dynamics. For this purpose, consider the probing beam as composed of a succession of segments of duration Δt . The field is in a coherent state, and hence factors in a product state of coherent states occupying each segment of the beam. The continuous measurement on the

probe beam after interaction with the cavity field now separates in the detection on each individual segment of light, and assuming an incident coherent state with a real field amplitude, the phase shift is registered by balanced homodyne detection of the phase-quadrature component by means of interference with a local oscillator field.

The interaction between the cavity field and a single segment of light is governed by the unitary operator $U = e^{-iM' \hat{n} \hat{n}_p}$, where M' is a measure of the coupling strength. We assume that each segment of the probe beam is in a coherent state with a large mean number of photons $\Phi\Delta t$, where Φ is the photon flux. Therefore, we can write $\hat{a}_p = \sqrt{\Phi\Delta t} + \hat{a}'_p$ and expand the time evolution operator to lowest order in the quantum fluctuations, $U = e^{-i\beta \hat{n} \hat{x}_p}$, where $\beta = 2M' \sqrt{\Phi\Delta t}$, and $\hat{x}_p = (\hat{a}'_p + \hat{a}'_p^\dagger)/2$. The interaction implies a displacement of the probe p quadrature proportional to the cavity photon number, and it is thus useful to expand the joint cavity and probe field state in the corresponding eigenstate basis, $|\Psi_{\text{in}}\rangle = \sum_n c_n |n\rangle \int dp_p \pi^{-1/4} e^{-p_p^2/2} |p_p\rangle$, so that the state after interaction becomes

$$|\Psi_{\text{out}}\rangle = \sum_n c_n |n\rangle \int dp_p \pi^{-1/4} e^{-(p_p - \beta n)^2/2} |p_p\rangle. \quad (1)$$

At this stage, p_p is measured, an arbitrary outcome is obtained according to the probability distribution,

$$f(p_p) = \pi^{-1/2} \sum_n |c_n|^2 e^{-(p_p - \beta n)^2}, \quad (2)$$

and the projection of (1) on the corresponding p_p eigenstate, yields the updated state of the cavity field,

$$|\Psi_c(p_p)\rangle = \mathcal{N}(\beta, p_p) \sum_n c_n e^{-(\beta n - p_p)^2/2} |n\rangle, \quad (3)$$

where $\mathcal{N}(\beta, p_p)$ is a normalization factor. When we model continuous probing, the parameter β is infinitesimal, and the effect of the interaction is merely to shift the Gaussian probability distribution for p_p by $\beta\langle n \rangle$. The update of the cavity field state after measurement is also infinitesimal due to the weak n dependence of the exponential factor in (3). The random detection can be modelled by a Wiener noise process, and the conditioned dynamics under continuous measurements can be brought on the form of an Itô stochastic master equation (SME) [7, 11]:

$$d\hat{\rho}(t) = M \mathcal{D}[\hat{n}]\hat{\rho}(t) dt + \sqrt{M\eta} \mathcal{H}[\hat{n}]\hat{\rho}(t) dW(t), \quad (4)$$

with $\mathcal{D}[\hat{X}]\hat{\rho} \equiv \hat{X}\hat{\rho}\hat{X}^\dagger - 1/2(\hat{X}^\dagger\hat{X}\hat{\rho} + \hat{\rho}\hat{X}^\dagger\hat{X})$ and $\mathcal{H}[\hat{X}]\hat{\rho} \equiv \hat{X}\hat{\rho} + \hat{\rho}\hat{X}^\dagger - \text{Tr}[(\hat{X} + \hat{X}^\dagger)\hat{\rho}]\hat{\rho}$. In (4) $M = 2M'^2\Phi$ denotes the measurement strength and $\eta \in [0, 1]$ represents the quantum efficiency of the detection. The *innovation process*, i.e., the difference between the actually observed p_p and its quantum mechanical expectation value with the current quantum state of the cavity field,

is described by a Wiener process [18], $dW(t)$. This difference is due to the shot noise in photo detection.

While the continuous measurement described above will eventually collapse the system on one of the Fock states present in the initial state, an important initial step of our scheme is to evolve the system towards a *given* Fock state. In Ref. [11], Geremia showed how to use the information gradually obtained about n by the detection record to feed coherent radiation into the cavity which in- or decreases the total photon number in a controllable manner. This feedback is described by adding to (4) terms that describes evolution under the Hamiltonian $\hat{H}_{\text{FB}}(t) = G e_f \hat{x}$. Here $\hat{x} = (\hat{a} + \hat{a}^\dagger)/2$ is the cavity field quadrature operator, G is the feedback gain factor, and e_f is the feedback policy function, that we take to depend on appropriate expectation values for the field. A natural choice for the feedback policy function is $e_f(\langle \hat{n} \rangle) = n^* - \langle \hat{n} \rangle$, where n^* is the desired photon number [11]. The feedback Hamiltonian causes a displacement of the field quadrature operator $\hat{p} = (\hat{a} - \hat{a}^\dagger)/(2i)$. The feedback is proportional to $n^* - \langle \hat{n} \rangle$, and a state with negative $\langle \hat{p} \rangle$ can be shifted to larger negative values of $\langle \hat{p} \rangle$ and hence typically a larger $\langle \hat{n} \rangle$, if desired.

The functioning of our complete scheme is illustrated in Fig. 1(a-e). We find heuristically (for $n^* \simeq 10$) that the following protocol has a high success rate: At time $t = 0$ we start with the electromagnetic vacuum (a) and we apply the Geremia Fock state feedback protocol towards n^* , but only until the quadrature $\langle \hat{p} \rangle < (n^* - 1)^{1/4} - \sqrt{n^*}$. At that time the Husimi Q -function looks like a crescent in position-momentum phase space (b). The state is now shifted towards the positive value $\langle \hat{p} \rangle = 0.9\sqrt{n^*}$ (c) and at that time we start again to observe (without feedback) the photon number in the system until the desired state is found (d). Finally, the state is shifted to a symmetric state around the centre of the phase space (e). We stop the action of the probing field when the maximum value of the Husimi Q -function along the p quadrature axis is below some fixed value δ (typically $\delta \leq 0.005$).

The protocol does not work in every run of the simulation/experiment. When we start the measurement on the crescent shape state it sometimes happens that the state collapses into a quasi coherent state [19], and sometimes the state dynamics becomes unstable. Since we have access to the density matrix conditioned on the measurement outcome, we know if the collapse takes place, and this problem is partially solved by starting over again to generate a new crescent state with the number state feedback generator. The instability problem is solved in our simulations by applying a not too fast ramp of increased measurement strength $M(t)$, controlled in the experiment by the probe laser power [11]. In our protocol it is important that the probing laser is not switched on too fast, but it is also important that it is switched off quickly to not perturb the state when it has been created

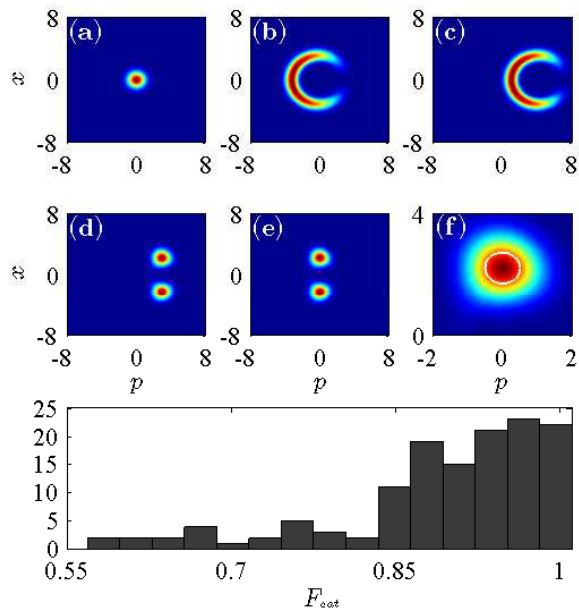


Figure 1: (Color online) Time evolution of the Husimi Q -function for a single successful realization of the linear superposition state ($\eta = 1$, $\kappa = 0$, and $n^* = 10$). In (f) the positive x component of the Husimi Q -function in (e) is magnified. The white ring in (f) indicates a contour for the choice of displaced squeezed state $|\alpha, \zeta\rangle$ in (5) that yields the best overlap with our state. The lower panel shows the histogram of the fidelity for 135 simulations with $n^* = 10$, $\kappa = 0$, and $\eta = 1$.

($t_{\text{switch-on}} \sim 200$ ns, $t_{\text{switch-off}} \sim 1 - 2$ ns for $M = 2.12$ MHz). Using these strategies and allowing a maximal production time of $10 M^{-1}$, we observed a success probability for the production of a quantum superposition state of 51% for $n^* = 5$, 69% for $n^* = 8$, and 77% for $n^* = 10$. Those results are obtained in the ideal situation of perfect detector efficiency and no cavity decay.

Our protocol does not automatically favor a superposition of coherent states, and we have investigated to which extent, the state produced can be written as a superposition of two Gaussian, minimum uncertainty states in the position-momentum phase space. As a way to quantify the quality of the state we use the optimal overlap fidelity

$$\mathcal{F}_{\text{sup}} := \max_{\zeta, \alpha, \phi} \{ \langle \Psi(\zeta, \alpha, \phi) | \hat{\rho} | \Psi(\zeta, \alpha, \phi) \rangle \}, \quad (5)$$

where $|\Psi(\zeta, \alpha, \phi)\rangle = \mathcal{N}(\zeta, \alpha, \phi) (|\alpha, \zeta\rangle + e^{i\phi} |-\alpha, \zeta^*\rangle)$, and where $\zeta = r e^{i\theta}$ is a squeezing parameter, $\alpha = x + iy$ is a displacement parameter, and $\mathcal{N}(\zeta, \alpha, \phi)$ is a normalization factor. The optimal superposition state parameters (α, ζ, ϕ) can be determined from the detection record in every run of the experiment. The results of 135 attempts to produce such quantum superposition states are summarized in the lower panel of Fig. 1, which provide an average fidelity of about 90%. The success probability for $n^* = 10$ does not change appreciably when a cavity

decay rate of $\kappa = 0.005 M$ and finite detector efficiency $\eta = 0.8$ are taken into account in our simulations, but the average fidelity decreases to 70%. Note that in our family of test superposition states we allow a relative phase ϕ . This phase is known to the experimenter based upon the detection record, but it is not under straightforward experimental control.

We will now explain our quantitative findings. We have found numerically that the crescent shaped state of Fig. 1(b), which is produced with a high success probability, is very close to the so-called crescent state of Ref. [20]. These states are eigenstates of the non-Hermitian operator $\hat{n} - 2i|\xi\rangle\langle\hat{x}$ [20]. When $|\xi| \rightarrow 0$ the eigenstate is close to a Fock state, while for $|\xi| \gg 1$ it is a coherent state. We now insert this state in Eq. (1) and we can semi-analytically follow the effect of probing, without applying any feedback. Since the measurement is of quantum non-demolition type, the equations (1-3) discussed for infinitesimal temporal segments, also apply for the accumulated effect of measuring on the probe field for an extended period of time. The parameter β is then larger, so that the probability distribution (2) for the p_p observable for a long time interval is no longer well approximated by a Gaussian. Instead, \hat{p}_p provides a weak measurement of \hat{n} , which according to Eq. (1) would become a projection in the limit $\beta \rightarrow \infty$. Figure 2(a) shows a plot of the p_p probability distribution $f(p_p)$ obtained for a typical probing time, corresponding to $\beta = 0.2$, for the crescent state. We identify three regions on the curves: (I) a maximum for small p_p , which is rather independent of n^* , (II) a central region where $f(p_p)$ decreases, and (III) a second maximum at $p_p \sim n^*$ followed by a rapid decay. Since \hat{p}_p measures the cavity photon number \hat{n} , the appearance of the three regions can be qualitatively understood in terms of the n distribution of the state or, more illustrative, in terms of the Husimi Q -function. Fock states are ring-shaped in phase space and in Fig. 2(c) and 2(d) we plot the displaced crescent state together with the region borders identified from Fig. 2(a) for $n^* = 8$ and for $n^* = 10$. It is seen that region (I) corresponds to the part of the state close to the origin. By increasing n^* , the weight in this region will only change slightly. In region (II) the ‘‘arms’’ of the crescent state are more or less radial in phase space while in region (III) they come together again. When n^* is increased, the crescent state becomes larger and the border between region (II) and (III) must move to larger radii, i.e. larger p_p .

From the phase space plots it is to be expected that region (II) is where a weak n measurement will cut out two well separated portions of the Husimi Q -function. This is confirmed by Fig. 2(b), which shows the maximum value of the post-measurement Husimi Q -function on the p -axis as a function of the measured p_p . We see that in the central region (II), the state produced has very small values of the Husimi Q -function on the p -axis, while the surrounding regions (I) and (III) are clearly not useful

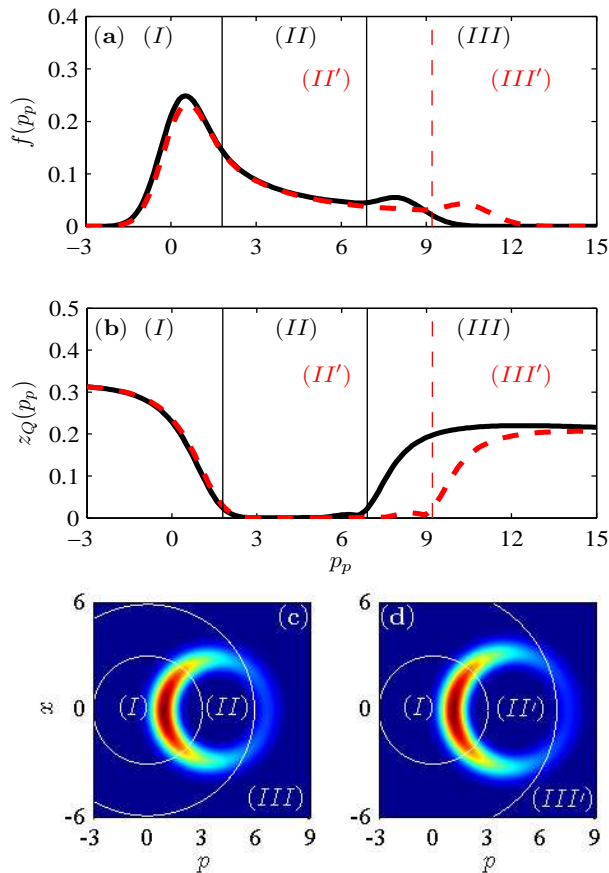


Figure 2: (Color online) (a) Probability distribution $f(p_p)$ for the outcome of the measurement of the probing field quadrature \hat{p}_p . (b) Maximum value of the Husimi Q -function $Q(x=0, p)$ plotted as a function of the measurement outcome p_p . The black (continuous) lines correspond to $n^* = 8$ while the red (dashed) ones to $n^* = 10$. In (c) and (d) are shown the corresponding Husimi Q -functions of the displaced crescent state together with the region borders identified from (a) and (b). In all pictures $\beta = 0.2$ has been taken.

for our purpose. Since the second maximum in Fig. 2(a) moves further to the right with increasing n^* , the central region (II) with the successful outcomes becomes larger and this explains that our protocol works better for larger n^* .

It should be noticed that the semi-analytical model based on the crescent state [20] suggests that the optimal superposition state parameters (α, ζ, ϕ) be uniquely determined by n^* , the duration of the final probing stage, and the corresponding integrated signal p_p . In an experiment, this is much easier than the numerical optimization based upon the solution of the SME (4).

In conclusion we have proposed to generate non-classical states of light in a cavity by using quantum measurements and feedback. A protocol for production of highly non-classical superposition states with high fi-

delity and success probability was proposed. We are currently working on the generalization of the ideas presented in this Letter to the generation of similar states of atomic ensembles.

The authors acknowledge financial support from the European Union Integrated Project SCALA. A. N. acknowledges R. J. Hendricks and Z. Hradil for useful information, U.V.P. acknowledges financial support by the Danish Natural Science Research Council, and K.M. acknowledges support of the ONR MURI on quantum metrology with atomic systems.

* E-mail: negretti@phys.au.dk

- [1] G. Chen, D. A. Church, B.-G. Englert, C. Henkel, B. Rohwedder, M. O. Scully, and M. S. Zubairy, in *Quantum Computing Devices*, (Chapman & Hall/CRC, Boca Raton, 2006).
- [2] P. Treutlein, T. W. Hänsch, J. Reichel, A. Negretti, M. A. Cirone, and T. Calarco, *Phys. Rev. A* **74**, 022312 (2006).
- [3] J. M. Geremia, J. K. Stockton, and H. Mabuchi, *Science* **304**, 270 (2004).
- [4] B. Julsgaard, J. F. Sherson, J. Fiurášek, J. I. Cirac, and E. S. Polzik, *Nature* **432**, 482 (2004).
- [5] J. F. Sherson, H. Krauter, R. K. Olsson, B. Julsgaard, K. Hammerer, J. I. Cirac, and E. S. Polzik, *Nature* **443**, 557 (2006).
- [6] A. S. Sørensen, and K. Mølmer, *Phys. Rev. Lett.* **91**, 097905 (2003).
- [7] H. M. Wiseman, and G. J. Milburn, *Phys. Rev. A* **49**, 4110 (1994).
- [8] V. Belavkin, *Rep. Math. Phys.* **43**, A405 (1999).
- [9] H. Carmichael, *An Open Systems Approach to Quantum Optics*, Lecture Notes in Physics, (Springer, Berlin, 1993).
- [10] J. Dalibard, Y. Castin, and K. Mølmer, *Phys. Rev. Lett.* **68**, 580 (1992).
- [11] J. M. Geremia, *Phys. Rev. Lett.* **97**, 073601 (2006).
- [12] M. Yanagisawa, *Phys. Rev. Lett.* **97**, 190201 (2006).
- [13] E. Knill, R. Laflamme, and G. Milburn, *Nature* **409**, 46 (2001).
- [14] D. Leibfried, E. Knill, S. Seidelin, J. Britton, R. B. Blakestad, J. Chiaverini, D. B. Hume, W. M. Itano, J. D. Jost, C. Langer, R. Ozeri, R. Reichle, and D. J. Wineland, *Nature* **438**, 639 (2005).
- [15] J. M. Raimond, M. Brune, and S. Haroche, *Phys. Rev. Lett.* **79**, 1964 (1997).
- [16] A. Ourjoumtsev, H. Jeong, R. Tualle-Brouri, and P. Grangier, *Nature* **448**, 784 (2007).
- [17] S. Gupta, K. L. Moore, K. W. Murch, and D. M. Stamper-Kurn, *ArXiv:0706.1052*.
- [18] L. Bouten, R. van Handel, and M. James, *SIAM J. Control Optim.* (2007), to appear, *arXiv:math/0601741*.
- [19] W. H. Zurek, S. Habib, and J. P. Paz, *Phys. Rev. Lett.* **70**, 1187 (1993).
- [20] Z. Hradil, *Phys. Rev. A* **44**, 792 (1991).